J Mater Sci (2008) 43:4921–4928
DOI 10.1007/s10853-008-2716-9

Phenomenological description of thermomechanical behavior of shape memory alloy

Jun-Yan Liu · Hao Lu · Jun-Mei Chen · Combescure Alain · Tong Wu

Received: 6 July 2007 / Accepted: 12 May 2008 / Published online: 30 May 2008

Abstract On the basis of a thermomechanical phenomenological model, we analyze the thermomechanical behavior of polycrystalline NiTi. Pseudoelastic response and strain-temperature response under fixed stress are studied by using finite element simulation. Calculated mechanical and thermal hysteresis behaviors of NiTi sheet are in good agreement with those observed experimentally. Hardening in stress–strain hysteresis loop and sharp change of strain in strain-temperature hysteresis loop are described by numerical simulation. The result from thermomechanically coupled calculation shows the phenomenon that phase transition occurs by nucleation and propagation of transformation fronts.

Introduction

In martensitic transition, atoms of parent phase which has higher crystallographic symmetry always move cooperatively by shear-like mechanism and martensitic phase which has lower symmetry is formed. In reverse transformation, martensite can revert to parent phase. Under presence of suitable thermomechanical load, it is the diffusionless, reversible martensitic transition in material that leads to the technologically-important properties of pseudoelasticity and shape-memory in shape memory alloy.

There are a lot of experimental researches on martensitic transition in shape memory alloy. In the experiments on pseudoelasticity of Ni–Ti wires, Shaw and Kyriakides observed that martensitic transition did not occur homogeneously in their specimens [1]. In their further researches, they found that there were apparent temperature changes in specimens caused by the latent heat of phase transformation. Moreover, their investigations showed that the phase transition was a process of nucleation and propagation of transformation fronts [2]. The phenomenon of temperature changes was also observed by Rodriguez et al. in their experiments on Cu–Al–Ni single crystal [3]. Besides that, temperature changes can result in an apparent hardening in nominal stress–strain response [4].

The model of martensitic transition in shape memory alloy could be subdivided into the following categories [5]: (1) Ginzburg-Landau or phase field theory; in phase field theory, the formation of a complicated microstructure consisting of austenite and many martensitic variants can be described. Interfaces between austenite and martensitic variants, as well as between martensitic variants appear as solutions of the evolution of equations for the order parameters. (2) thermomechanical phenomenological model; in this model, some researchers introduced the volume fraction of martensitic variants and treated material with phase transition as composite with varying volume fractions. (3) Elastoplastic models with strain softening applied to the simulation of martensitic transformation; strain softening leads to the formation of domains with localized strains that resemble microstructures observed during phase transitions. In this model, by modeling inhomogeneous deformations, the evolution of martensite is simulated.

By introducing the volume fractions of martensitic variants as internal variables, V. I. Levitas et al. modeled martensitic phase transformations within thermodynamic framework [5, 6]. On the basis of their work, we explicitly

J.-Y. Liu · H. Lu (✉) · J.-M. Chen
Materials Science and Engineering School, Shanghai Jiaotong University, Shanghai 200030, China
e-mail: shweld@sjtu.edu.cn

C. Alain · T. Wu
LaMCoS, INSA-Lyon, 69621 Villeurbanne, France

introduced the thermal and transformational part of Helmholtz free energy and reformulated the thermomechanical model. In this article, thermomechanical behavior of polycrystalline NiTi sheet is analyzed by coupling phase transition to temperature evolution. Stress–strain hysteresis loop and strain-temperature hysteresis response are simulated by using finite element method.

The plan of this article is as follows: In Sect. 2, we summarize the constitutive model for martensitic transition in elastic material, which includes: kinetic equation for phase transition, constitutive equation for stress and heat equation. In Sect. 3, thermomechanical behavior of polycrystalline NiTi sheet is simulated. The stress–strain responses under different applied strain rates and the strain-temperature response under different applied stress levels are computed by performing finite element calculation. At last, in Sect. 4, we present our conclusions.

Constitutive model

Thermomechanical model

In this section, we present the summarization of the constitutive model for martensitic transition in elastic material. For more details regarding the derivation of it, please refer to J.Y. Liu et al. [7]. Our model is based on the homogenization on representative volume. Here, we take a single crystal of austenite as a representative volume, which includes many different martensitic variants corresponding to different habit planes and shear directions.

We use the additive decomposition of the total strain, $\boldsymbol{\varepsilon}$, into elastic $\boldsymbol{\varepsilon}_e$ and transformation, $\boldsymbol{\varepsilon}_t$, parts, that is

$$\boldsymbol{\varepsilon} = \boldsymbol{\varepsilon}_e + \boldsymbol{\varepsilon}_t \tag{1}$$

The volume fraction of each of martensitic variant ξ_i, $i = 1,\ldots m$ is introduced into the model as internal variable. Moreover, as for the transformation strain $\boldsymbol{\varepsilon}_t$, the following equation exists $\boldsymbol{\varepsilon}_t = \sum_{j=1}^{m} \boldsymbol{\varepsilon}_{ti}\xi_i$, where $\boldsymbol{\varepsilon}_{ti}$ is the transformation strain that transforms the crystal lattice of the austenite into the crystal lattice of martensitic variant i [8].Then from the second law of thermodynamics in the form of Clausius–Duhem inequality, the dissipation inequality shown as follows can be deduced:

$$\begin{aligned}\Phi &= \sum_{i=1}^{m}(\boldsymbol{\sigma} : \boldsymbol{\varepsilon}_{ti} - \frac{\partial\psi}{\partial\xi_i})\dot{\xi}_i - q\cdot\frac{\overline{grad}T}{T} \\ &= \sum_{i=1}^{m} X_i\dot{\xi}_i - \vec{g}\cdot\vec{q}/T \geq 0\end{aligned} \tag{2}$$

where ψ is the Helmholtz free energy of a representative volume, T is the temperature, $\boldsymbol{\sigma}$ is the stress, $\vec{q}$ is the heat flux, $\overline{grad}T$ is the temperature gradient, $\vec{g} = \overline{grad}T$ and ":" represents contraction of tensor over two indices. X_i is the thermodynamic force conjugate to the internal variable ξ_i and it's expression is:

$$X_i = \boldsymbol{\sigma} : \boldsymbol{\varepsilon}_{ti} - \frac{\partial\psi}{\partial\xi_i} \tag{3}$$

Free energy

In the model, the Helmholtz free energy is assumed to be of the form:

$$\psi(\boldsymbol{\varepsilon}_e, T, \xi_i) = \psi^e(\boldsymbol{\varepsilon}_e, T, \xi) + \psi^{\text{th}}(T, \xi) + \psi^p(T, \xi_i) \tag{4}$$

here:

(1) ψ^e is the strain energy, and is given by

$$\psi^e(\boldsymbol{\varepsilon}_e, T, \xi) = \frac{1}{2}\boldsymbol{\varepsilon}_e : \mathbb{C}(\xi) : \boldsymbol{\varepsilon}_e - (T - T_a)\mathbf{A}(\xi) : \mathbb{C}(\xi) : \boldsymbol{\varepsilon}_e \tag{5}$$

where $\xi = \sum_{i=1}^{m}\xi_i$ is the volume fraction of martensite, $\mathbb{C}(\xi)$ is the symmetric positive-definite elastic tensor at the reference temperature T_a, $\mathbf{A}(\xi)$ is the symmetric thermal expansion tensor at T_a.

(2) ψ^p is the energy of transformation, and is given by:

$$\psi^p(T, \xi_i) = \frac{\lambda_0}{T_0}(T - T_0)\xi + g_0\xi\xi_0 \tag{6}$$

where T_0 is the phase equilibrium temperature, λ_0 is the latent heat of martensitic transition at T_0. Material parameter g_0 characterizes the interactions between austenite and martensite, and $g_0 > 0$. ξ_0 is the volume fraction of austenite, and $\xi_0 = 1 - \xi = 1 - \sum_{i=1}^{m}\xi_i$.

(3) ψ^{th} is the thermal energy, and is given by

$$\psi^{\text{th}}(T, \xi) = c(T - T_a) - cT\ln(\frac{T}{T_a}) \tag{7}$$

where $c > 0$ is the specific heat.

In this article, we assume that the elastic and thermal expansionary properties of austenite and martensite are identical and isotropic [7, 9], that is

$$\mathbb{C}(\xi) = \mathbb{C}, \mathbf{A}(\xi) = \mathbf{A} = \alpha\mathbf{I}$$

where α is thermal expansion efficient and $\mathbf{I}$ is unit tensor. Hence Eq. 5 could be reduced to as follows:

$$\psi^e(\boldsymbol{\varepsilon}_e, T, \xi) = \frac{1}{2}\boldsymbol{\varepsilon}_e : \mathbb{C} : \boldsymbol{\varepsilon}_e - (T - T_a)\mathbf{A} : \mathbb{C} : \boldsymbol{\varepsilon}_e \tag{8}$$

Constitutive equation for stress

The constitutive equation for stress is as follows:

$$\boldsymbol{\sigma} = \frac{\partial\psi}{\partial\boldsymbol{\varepsilon}_e} = \mathbb{C} : [\boldsymbol{\varepsilon}_e - \mathbf{A}(T - T_a)] \tag{9}$$

Model for phase transition

By defining $\dot{\xi}_{ij}$ as the rate of change of the volume fraction ξ_i due to a transition from phase (or variant) j to i, the kinetic equation of martensitic transition is shown as follows:

$$\begin{aligned} |X_{ij}| > k_{ij} &\Rightarrow \dot{\xi}_{ij} = \lambda_{ij} sign(X_{ij})(|X_{ij}| - k_{ij}) \\ |X_{ij}| \le k_{ij} &\Rightarrow \dot{\xi}_{ij} = 0 \end{aligned} \tag{10}$$

where X_{ij} is the driving force for phase transformation. When $j = 0$, $X_{i0} = X_i$ is the driving force for transition from austenite to martensitic variant i (if $X_{i0} > 0$) or for transition from martensitic variant i to austenite (if $X_{i0} < 0$). When $j \neq 0$, $X_{ij} = X_i - X_j$ is the driving force for transition from martensitic variant j to variant i (if $X_{ij} > 0$) or for transition from martensitic variant i to variant j (if $X_{ij} < 0$). k_{ij} is the given dissipative threshold, λ_{ij} are kinetic coefficients.

Heat equation

From the first law of thermodynamics and the expression for Helmholtz free energy, the deduced heat equation is:

$$c\dot{T} - k\Delta T = \sum_{i=1}^{m} X_i \dot{\xi}_i + T\left(\frac{\lambda_0}{T_0}\dot{\xi} - \mathbf{A} : \mathbb{C} : \dot{\boldsymbol{\varepsilon}}_e\right) - r \tag{11}$$

where r is the heat supply, k is the coefficient of thermal conductivity.

Finite element simulation of thermomechanical behavior of NiTi

By using our model, we have analyzed the martensitic transition in single crystal of shape memory alloy. The simulated results have a good agreement with those observed experimentally [7]. For polycrystalline materials, a widely used average scheme is based on the Taylor assumption that the local deformation in each crystal is homogeneous and identical to the macroscopic deformation at the continuum material point [10, 11]. Moreover, the calculated responses of shape memory alloy by using this assumption have a good agreement with experiments and that of full element calculations which do not make this assumption [11]. For computational efficiency, we also use this assumption to analyze the thermomechanical behavior of polycrystalline NiTi shape memory alloy on the basis of our model. The finite element algorithm for the solution of martensitic transition is the Newton–Raphson iterative scheme [12]. All the FEM calculation source codes are generated by using finite element computer program FEPG.

From the crystallographic theory of martensitic transition, phase transformation in NiTi can occur in 192 transformation systems [13]. However, it is not clear whether all the systems are operative under thermomechanical loading. Here, we select 24 type II transformation systems used by a variety of researchers[14, 15].Therefore, the value of m, which denotes the number of martensitic variants in the model, is equal to 24, that is $m = 24$.

From the crystallographic theory, the transformation strain produced by *ith* martensitic variant can be described as follows [8, 15, 16]:

$$\boldsymbol{\varepsilon}_{ti} = \gamma_t^i \mathbf{R} = \frac{1}{2}\gamma_t^i(\mathbf{en} + \mathbf{ne}) \tag{12}$$

where γ_t^i is material parameter, $\mathbf{R}_i$ is the orientation tensor of the martensite variant i, unit vector **e** denotes the average "transformation" direction, **n** is a unit vector normal to the austenite-*ith*martensitic variant interface. In general, e is not perpendicular to n. As far as NiTi is concerned, the components of **e** and **n** for 24 transformation systems with respect to orthonormal basis associated with the cubic austenite crystal lattice are listed in Table 1 [14].

Table 1 Transformation systems

i	n^1	n^2	n^3	e^1	e^2	e^3
1	−0.8888	−0.4045	0.2153	0.4343	−0.4878	0.7576
2	−0.8888	0.4045	0.2153	0.4343	0.4878	0.7576
3	−0.8888	0.2153	−0.4045	0.4343	0.7576	−0.4878
4	−0.8888	0.2153	0.4045	0.4343	0.7576	0.4878
5	−0.8888	−0.2153	0.4045	0.4343	−0.7576	0.4878
6	−0.8888	−0.2153	−0.4045	0.4343	−0.7576	−0.4878
7	−0.8888	0.4045	−0.2153	0.4343	−0.4878	−0.7576
8	−0.8888	−0.4045	−0.2153	0.4343	−0.4878	−0.7576
9	0.4045	−0.8888	0.2153	0.4878	0.4343	0.7576
10	−0.4045	−0.8888	0.2153	−0.4878	0.4343	0.7576
11	0.2153	−0.8888	−0.4045	0.7576	0.4343	−0.4878
12	0.2153	−0.8888	0.4045	0.7576	0.4343	0.4878
13	−0.2153	−0.8888	0.4045	−0.7576	0.4343	0.4878
14	−0.2153	−0.8888	−0.4045	−0.7576	0.4343	−0.4878
15	0.4045	−0.8888	−0.2153	0.4878	0.4343	−0.7576
16	−0.4045	−0.8888	−0.2153	−0.4878	0.4343	−0.7576
17	0.2153	0.4045	−0.8888	0.7576	0.4878	0.4343
18	0.2153	−0.4045	−0.8888	0.7576	−0.4878	0.4343
19	0.4045	0.2153	−0.8888	0.4878	0.7576	0.4343
20	−0.4045	0.2153	−0.8888	−0.4878	0.7576	0.4343
21	0.4045	−0.2153	−0.8888	0.4878	−0.7576	0.4343
22	−0.4045	−0.2153	−0.8888	−0.4878	−0.7576	0.4343
23	−0.2153	0.4045	−0.8888	−0.7576	0.4878	0.4343
24	−0.2153	−0.4045	−0.8888	−0.7576	−0.4878	0.4343

Moreover, the value of γ_t^i for all transform systems are same and equal to 0.1308 [13], that is

$$\gamma_t^i \equiv \gamma_t = 0.1308 \quad \text{for } i = 1, \ldots 24$$

Simulation of pseudoelastic response

As an important characteristic thermomechanical behavior of shape memory materials, pseudoelasticity is a consequence of stress-induced martensitic transformation. In this section, we numerically simulate the stress–strain response of NiTi sheet specimen when tensile experiment is conducted at 300 K.

The geometry of our finite element model used in calculation is shown in Fig. 1a. The dimension of specimen is 10.0 × 1.0 × 0.2 mm. In our computation, the finite-element mesh is comprised of 500 three-dimensional 8-node elements, just as shown in Fig. 1b.

In the simulation of tensile experiment, displacements in three directions of one end of our model are all restrained, and the opposite end moves in tensile direction at a constant strain rate (± 3.0 × 10^{-5}/s) to simulate loading and unloading. Since the strain rate is very low, isothermal condition is adopted in calculation. In tensile experiment, the transition between different martensitic variants may occur during forward and reverse martensitic transformation. For simplicity, we only consider the transition between austenite and martensite, and neglect the contribution to free energy due to the interaction between austenite and martensite in finite element computation. Further, we assume that the kinetic coefficients for the transitions between austenite and different martensite variants are all the same constants. The value of dissipative thresholds for transitions are also assumed to be equal and constant. Therefore,

$$g_0 = 0, \quad \lambda_{i0} \equiv \lambda_{\text{ma}} = \text{const}, \quad k_{i0} \equiv k_{\text{ma}} = \text{const}$$

In our calculation, the value of Possion's ratio is 0.33[12]. The material parameters used are listed in Table 2 [11]. The parameters calibrated from experimental results are:

Elastic moduli: $E = 3.0 \times 10^4$ MPa,

Kinetic coefficient: $\lambda_{\text{ma}} = 0.9 \times 10^4$/MPa s.

Table 2 Material parameters of polycrystalline Ni–Ti sheet

λ_T (MJ/m^3)	T_0 (K)	k_{ma} (MJ/m^3)	c (MJ/m^3)	α ($\times 10^{-6}$/K)	k (W/mK)
110	271	4.7	2.1	6.6	13

The nominal stress–strain curve from finite element simulation is shown in Fig. 2, which has a good agreement with the experiment result observed by P. Thamburaja et al. [11]. From the calculated result, we could find that the stress–strain relationship under loading or unloading can be divided into three stages. At first, the deformation behavior of parent phase (austenite) under loading is elastic and conforms to Hooke's law. When the stress reaches a critical value ($\sigma_{\text{AM}}^{\text{th}}$), the strain increases under almost constant stress due to martensitic transition. After the phase transformation is finished, the elastic deformation of martensite happens. Upon unloading, one can make similar analysis on the evolution of the stress–strain relationship: the elastic deformation of martensite takes place until the stress decrease to a critical value

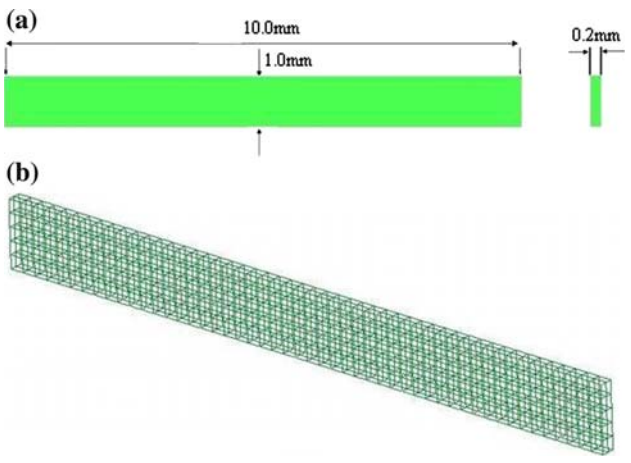

Fig. 1 (**a**) Geometry of the finite element model. (**b**) Undeformed finite-element mesh of the model using 500 three-dimensional elements

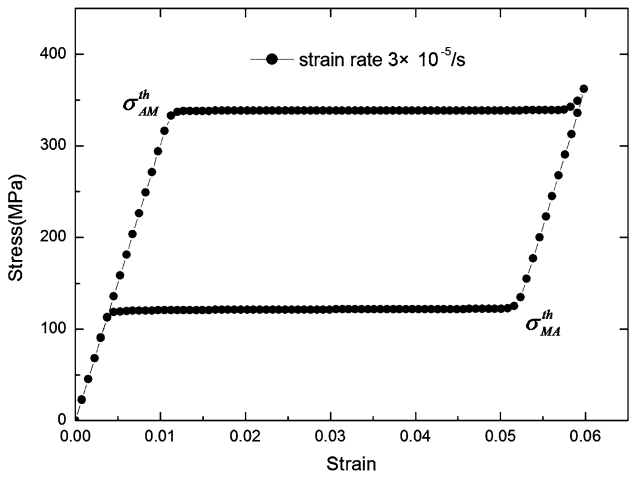

Fig. 2 Stress–strain curves from simulations of pseudoelastic tension experiments on NiTi sheet specimen under strain rate : 3.0 × 10^{-5}/s. The computation is conducted under isothermal condition

(σ^{th}_{MA}). Then the deformation takes place under almost constant stress during the transition from martensite to austenite. When the reverse transformation is finished, the elastic deformation of austenite is present. From Fig. 2, we also find that the critical stress value for forward and reverse transition are different: $|\sigma^{th}_{MA}| < |\sigma^{th}_{AM}|$. The hysteresis phenomenon in the pseudoelastic behavior is successfully described in the result from finite element simulation.

To analyze the interaction between phase transition and temperature variation, pseudoelastic responses of NiTi under three different strain rates (3.0×10^{-5}/s, 8.4×10^{-5}/s, 2.0×10^{-4}/s) are computed by thermomechanically coupled calculation. In calculation, we neglect the term $\mathbf{A} : \mathbb{C} : \dot{\boldsymbol{\varepsilon}}_e$ in Eq. 11. Since there is no inner heat supply, heat equation can be reduced to Eq. 13. As for the thermal boundary condition of finite element model, we take the ambient temperature and the initial temperature of specimen as 300 K in according to experiment. During tensile experiment, the ends of specimen are gripped. The convection conditions of them are worse. Therefore, for simplicity, we only apply convection conditions on the others four surfaces of finite element model. The convection coefficient used in calculation is $h = 12W/Km^2$ [11]

$$c\dot{T} - k\Delta T = \sum_{i=1}^{m} X_i \dot{\xi}_i + T\frac{\lambda_0}{T_0}\dot{\xi} \tag{13}$$

The stress–strain responses under three strain rates from calculation are shown in Fig. 3. The calculated highest and lowest temperatures of specimen during pseudoelastic deformation under three strain rates are listed in Table 3.

From Fig. 3, it can be found that when the applied strain rate is very low (3.0×10^{-5}/s), the result from coupled computation is similar to that under isothermal condition. When the strain rate is high, there is an apparent hardening response in the stress–strain curve. Moreover, the hardening and the width of hysteresis loop increase with the applied strain rate. Since we set $k_{i0} \equiv k_{ma} = \text{const}$ in calculation, the hardening response is entirely due to thermal effects associated with phase transformations. When the applied strain rate is small, there is enough time for heat transfer between specimen and its surroundings, so the temperature variation of specimen is also small (see Table 3). When the applied strain rate is high, because there isn't enough time for heat transfer, the temperature variation of specimen is high (see Table 3). Therefore, there is an apparent hardening in the stress–strain curve.

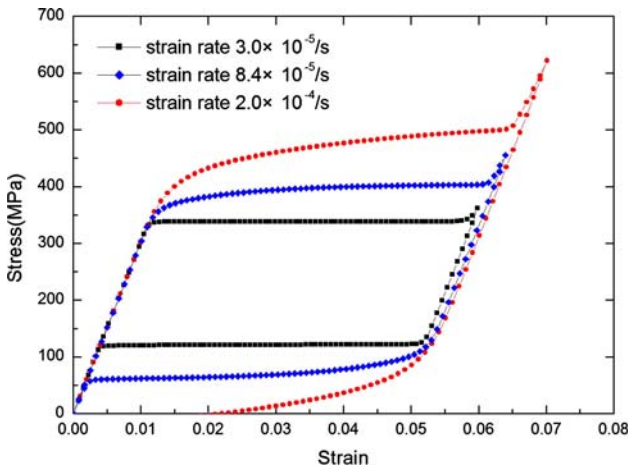

Fig. 3 stress–strain curves of NiTi from thermomechanically coupled simulation under three strain rate

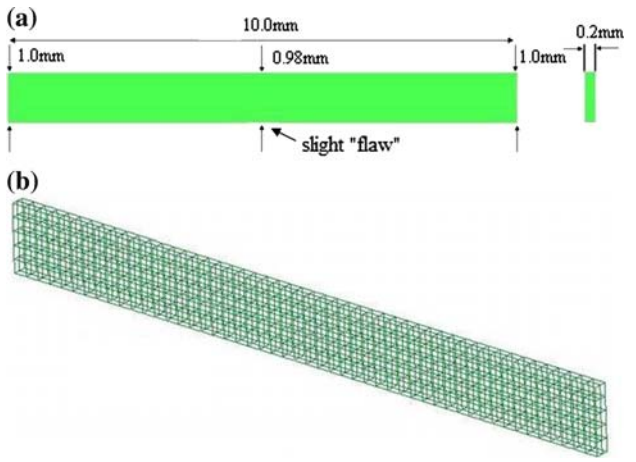

Fig. 4 (**a**) Geometry of the finite element model with a slight "flaw". (**b**) Undeformed finite-element mesh of the model using 500 three-dimensional elements. From the ends of the model to the mid section, the width is linearly tapered from 1.0 mm to 0.98 mm

Table 3 The highest and lowest temperature of specimen during tensile from thermomechanically coupled simulation under three strain rates

Strain rate	3.0×10^{-5}/s		8.4×10^{-5}/s		2.0×10^{-4}/s	
	Highest temperature	Lowest temperature	Highest temperature	Lowest temperature	Highest temperature	Lowest temperature
Temperature (K)	302.07	297.65	312.87	288.97	325.95	279.47

Another finite element model used in our calculation is shown in Fig. 4a. Comparing it with the model in Fig. 1, we can found that a slight "flaw" is introduced. The width at the center of finite element model in Fig. 4a is slightly narrower than that at two ends. There are slight tapers between the center and the ends. The "flaw" in this model is introduced to provide an initial site for phase transition. The finite-element mesh of this model is also comprised of 500 three-dimensional 8-node elements, just as shown in Fig. 4b.

By using the model with a slight "flaw," we analyze martensitic transition in tensile test. When the strain rate is 2.0×10^{-4}/s, calculated stress–strain response from thermomechanically coupled analysis is shown in Fig. 5a. In Fig. 5b, evolution of the contours of the martensite volume fraction at representative instances (a) through (l) keyed to Fig. 5a, during the forward and reverse transformations for the test at the highest strain rate, is shown.

From the calculated result (contour (a–f) in Fig. 5b), we can find that martensite first nucleates at the center of the specimen. Due to the slight flaw introduced in the calculated model, the width at the center is the narrowest. During loading, the stress at the center is greater. Therefore, stress-induced martensite first nucleates at this place. Moreover, it can also be found that the transformation fonts propagate to the two ends under further loading. The transformation fronts recede when the specimen is under unloading, just as shown in contours of (g–l) in Fig. 5b. The phenomenon that phase transition occurs by nucleation and propagation of front is qualitatively captured in our calculated results.

Simulation of strain-temperature response under fixed stress

In this section, we analyze the strain-temperature hysteresis response of polycrystalline NiTi. When shape memory alloy is subjected to a fixed stress, we could obtain a recoverable strain cycle by cycling temperature in a narrow range of temperature [11].

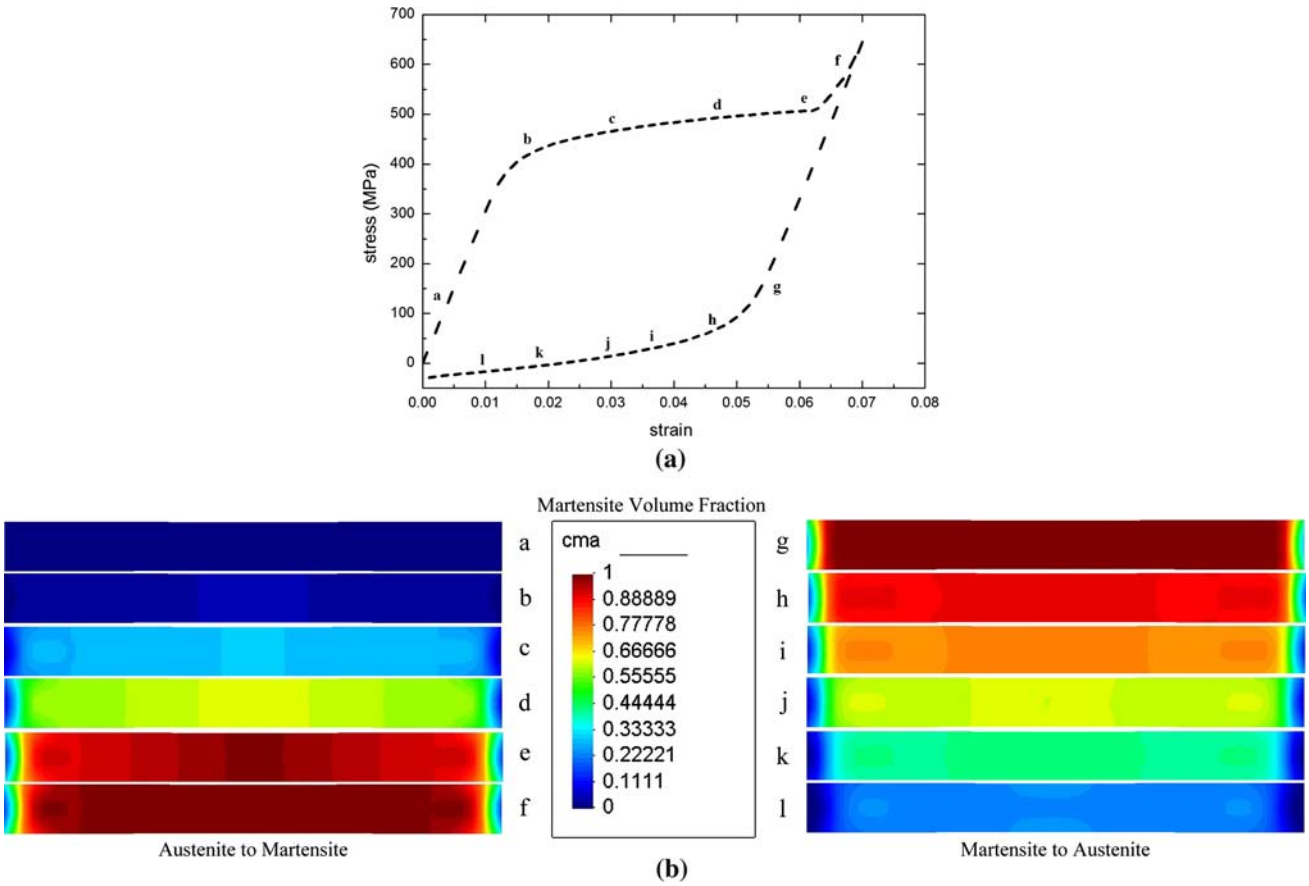

Fig. 5 (**a**) Stress–strain curve of NiTi from thermomechanically coupled simulation of pseudoelastic tension conducted at strain rate of 2.0×10^{-4}/s by using the model with a slight "flaw". (**b**) Contours of martensite volume fraction from simulation of pseudoelastic tension. The set of the contours on the left shows the transformation from austenite to martensite during forward transformation, while those on the right show the transformation from martensite to austenite during reverse transformation. The labels (a–l) are keyed to the stress–strain curve in (**a**). Note that because of the slight taper in the model, the austenite-to-martensite transition nucleates at the center and propagates toward two ends

In finite element simulation, we still study polycrystalline NiTi sheet specimen and the finite element model is shown in Fig. 1. In calculation, we first restrain all displacements of one end of the model and pull the opposite end in tensile direction. When stress increases to the requested level, we keep stress fixed and decrease temperature globally at a constant rate (0.016 K/s), and then increase it back at the same rate. After computation, the strain-temperature response in a temperature cycle is analyzed.

The material parameters used in calculation are listed in Table 2 [11]. The parameters calibrated from experimental results are:

Elastic moduli: $E = 3.0 \times 10^4$MPa,

Kinetic coefficient: $\lambda_{ma} = 0.4 \times 10^{-3}$/MPa s.

The calculated strain-temperature responses under two different fixed stress levels (150, 250 MPa) are shown in Fig. 6. The relation between temperature and volume fraction of martensite at the center point of the specimen is shown in Fig. 7.

From the calculated results, it can be found that in a temperature cycle under a fixed stress level, the strain-temperature response during heating or cooling can be divided into three stages: when the temperature is decreased from its initial level, the strain first decreases slightly from its initial value due to thermal contraction (The initial values of strain are different due to the different levels of applied axial stresses. For example, the initial strain is about 0.005 when the applied axial stress is 150 MPa). When the temperature is deceased to a critical value (for example, which is about 278 K when the fixed stress is 150 MPa), there is a sharp increase of the strain due to martensitic transition (see Fig. 7). After the phase

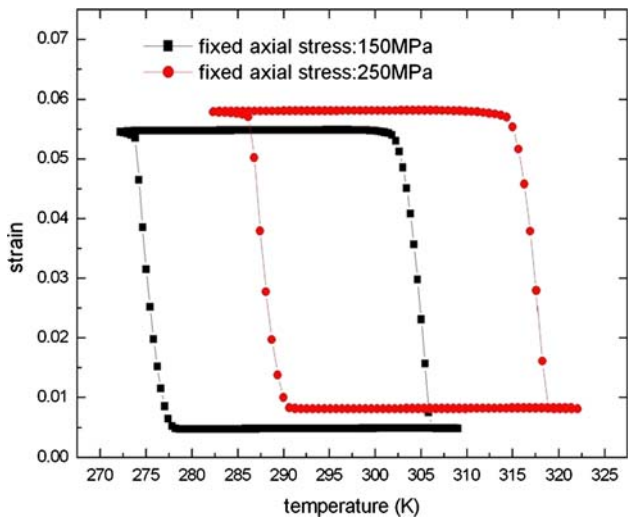

Fig. 6 Strain-temperature responses under two different fixed stresses (150, 250 MPa) from finite element simulation

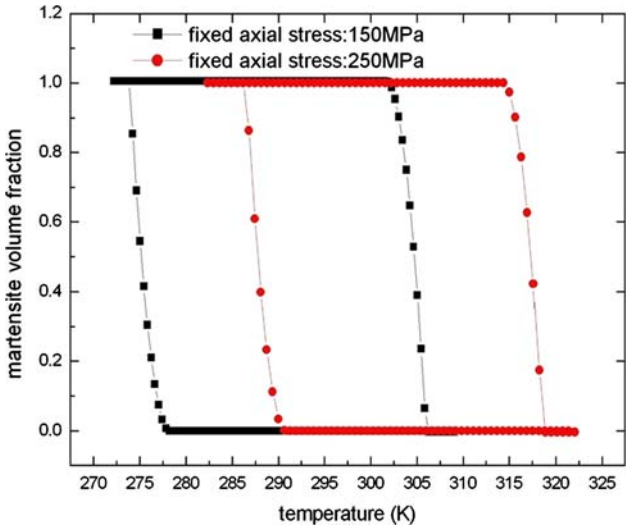

Fig. 7 Relations between temperature and martensite volume fraction at the center point of the specimen under two different fixed stresses (150, 250 MPa) from finite element simulation

transition is finished, the variation of strain is produced again only by temperature change. When heating, similar analysis can be made: in stage one, the variation of strain is produced by thermal expansion of martensite until the temperature is increased to a critical value. Then the reverse martensitic transition takes place (see Fig. 7), and the strain decreases sharply. After the reverse phase transition is finished, the thermal expansion of austenite results in a slight increase of the strain.

By comparing the strain-temperature responses under different fixed stress levels, we can find that the critical temperatures at which forward and reverse transformations take place are related to stress levels. When the fixed stress is increased, the temperatures at which forward and reverse transformations happen are also increased. The results from finite element simulation have a good agreement with the experimental results [11].

Conclusion

On the basis of the phenomenological model proposed in this article, the thermomechanical behavior of polycrystalline NiTi is analyzed. Pseudoelastic response and strain-temperature hysteresis response are simulated by finite element calculation. The computed results have a good agreement with those observed in experiments.

(1) The pseudoelastic response of polycrystalline NiTi is accurately described in the calculated result. In the thermomechanically coupled calculated results, stress–strain response under fixed temperature show a hardening, and the hardening increase with the

applied strain rates. The phenomenon that phase transition occurs by nucleation and propagation of transformation fronts is also captured.

(2) The strain-temperature hysteresis response is accurately described by numerical simulation. The characteristic that temperatures at which phase transition take place are different under different fixed stress levels is also explained well by the calculated results.

Acknowledgement This project is supported by the National Natural Science Foundation of China (Grant No.50475021).

References

1. Shaw JA, Stelios K (1995) J Mech Phys Solids 43:1243. doi:10.1016/0022-5096(95)00024-D
2. Shaw J, Kyriakides S (1997) Acta Mater 45:683. doi:10.1016/S1359-6454(96)00189-9
3. Rodriguez C, Brown LC (1980) Metall Trans A llA:147
4. Entemeyer D, Patoor E, Eberhardt A, Berveiller M (2000) Int J Plastic16:1269. doi:10.1016/S0749-6419(00)00010-3
5. Idesman AV, Levitas VI, Preston DL, Chao JY (2005) J Mech Phys Solids 53:495. doi:10.1016/j.jmps.2004.10.001
6. Levitas VI, Idesman AV, Preston DL (2004) Phys Rev Lett 93:105701. doi:10.1103/PhysRevLett.93.105701
7. Liu JY, Lu H, Chen JM, Zhang Z (2007) Mater Sci Eng A 448:204. doi:10.1016/j.msea.2006.10.053
8. Lexcellent C, Goo BC, Sun QP, Bernardini J (1995) Acta mater 44:3773. doi:10.1016/1359-6454(95)00452-1
9. Thamburaja P (2005) J Mech Phys Solids 53:825. doi:10.1016/j.jmps.2004.11.004
10. Taylor GI (1938) J Inst Metals 62:30
11. Thamburaja P, Anand L (2003) Acta mater 51:325. doi:10.1016/S1359-6454(02)00389-0
12. Simo J, Hughes T (1998) Computational inelasticity. Springer, New York
13. Hane K, Shield T (1999) Acta Mater 47:2603. doi:10.1016/S1359-6454(99)00143-3
14. Thamburaja P, Anand L (2002) Int J Plastic 18:1607. doi:10.1016/S0749-6419(02)00031-1
15. Thamburaja P, Pan H, Chau FS (2005) Acta mater 53:3821. doi:10.1016/j.actamat.2005.03.054
16. Fang D-N, Lu W, Yan W-Y, Inoue T, Hwang K-C (1999) Acta mater 47:269. doi:10.1016/S1359-6454(98)00303-6